THE ASTROPHYSICAL JOURNAL, 280:470–475, 1984 May 15

SUPERCLUSTER-SUPERCLUSTER INTERACTIONS

EDWARD J. SHAYA
Institute for Astronomy, University of Hawaii
Received 1983 April 1; accepted 1983 November 9

ABSTRACT

Monte Carlo simulations are made to determine the probability distribution of peculiar velocities and shear velocities of superclusters. Mass fluctuations on the scale of superclusters are represented as mass points distributed randomly in three dimensions. Accelerations and the components of the tidal tensor at the center of a spherical region due to the gravitation of masses exterior to the sphere are calculated. It is concluded that peculiar velocities greater than ~ 200 km s^{-1} are expected in a majority of superclusters if $\Omega \gtrsim 1$ and $N^{-1/3}/R_{\delta=1} = 3.2$, where N is the number density of substantial superclusters and $R_{\delta=1}$ is the mean supercluster radius at which δ, the fractional density excess internal to R, reaches unity. A peculiar velocity of ~ 300 km s^{-1} for our supercluster implies a 95% probability that $\Omega > 0.2$. A shear velocity of ~ 150 km s^{-1} at our position in the supercluster is expected if superclusters have mass excesses of $\sim 3 \times 10^{15}\ M_\odot$ ($\Omega \sim 1$) and are at a number density of 1 per (80 Mpc)^3. The distribution of tidal strengths in the direction of maximal distention is compared with self-gravitational forces in the outer regions of superclusters; tidal fields are found to strongly influence the low-density outer contours of superclusters.

The observed direction of motion of the Local Supercluster is found to be toward Hydra/Centaurus, the nearest large supercluster.

Subject headings: cosmology — galaxies: clustering — galaxies: redshifts

I. INTRODUCTION

The motion of the Local Supercluster with respect to the microwave background can be derived, in principle, by subtracting the solar motion with respect to the other galaxies in the Local Supercluster from the solar motion with respect to the microwave background. It has been noted (de Vaucouleurs *et al.* 1981) that the vector of our motion with respect to the blackbody radiation is not properly reflected in the radial velocities of our surrounding galaxies. A possible interpretation of this discrepancy is that dynamical interactions among superclusters are causing motions of several hundred kilometers per second.

A weighted average of measurements of the dipole moment of the 3 K background about the Sun (Clutton-Brock and Peebles 1981) is 380 ± 17 km s^{-1} in the direction $l = 269°$, $b = 56°$. Subtracting the solar motion with respect to galaxies with radial velocities less than 3000 km s^{-1} leaves a motion of this nearby region of 491 km s^{-1} toward $l = 290°$, $b = 19°$ for the determination of de Vaucouleurs *et al.* (1981) and 383 km s^{-1} toward $l = 291°$, $b = 1°$ for the determination of Aaronson *et al.* (solution 3.1, 1982). Both studies, therefore, indicate substantial motion of the entire supercluster roughly toward the Hydra/Centaurus Supercluster at $l \approx 285°$, $b \approx 25°$ (Chincarini and Rood 1979). The Hydra/Centaurus Supercluster comprises the Centaurus, Hydra I, and Antlia clusters plus several smaller clusters, all with redshifts in the range $2220 < v < 3600$ km s^{-1}. This entity skirts the Galactic plane; therefore, there may be other significant components associated with this supercluster that remain undetected because of obscuration. For now, we resort to statistical arguments to determine how reasonable it is that our supercluster has such a high velocity, regardless of the direction.

As the following analysis shows, motions of several hundred km s^{-1} are expected to arise between superclusters from the summed gravitational interactions of all nearby superclusters if (1) the "average" mass excess of superclusters is $\sim 10^{15}\ M_\odot$, and (2) the number density of these systems is (80 Mpc)$^{-3}$. If superclusters are more massive or numerous, or if clustering on scales larger than superclusters is significant, then greater typical velocities would be expected, and we would need to accept the hypothesis that our supercluster neighborhood is in an exceptionally rare arrangement that has generated an abnormally low velocity for the Local Supercluster.

Tidal distortions and rotation are yet another product of large scale clustering of matter. Superclusters typically reside only a few supercluster radii from one another. Therefore they are quite likely to undergo mutual tidal disturbances. For instance, Binggeli (1982) found that neighboring Abell clusters, separated by less than $\sim 60\ h^{-1}$ Mpc, strongly tend to "point to each other." Also, Tully (1982) found prominent clouds in the "halo" of the Local Supercluster to be prolate structures with their long axes directed toward the Virgo Cluster.

De Vaucouleurs (1958) and Aaronson *et al.* (1982) suggest the Local Supercluster is rotating with a velocity greater than 100 km s^{-1} at the position of the Local Group. A natural mechanism to explain this motion is the torque of the tidal field of neighboring superclusters. This mechanism was investigated by Peebles (1969), Thuan and Gott (1977), and Efstathiou and Jones (1979) to explain the origin of rotation of galaxies.

In § II the average value of the square of the acceleration at a given point, $\langle g^2 \rangle$, is derived analytically for power laws in the mass function for superclusters. In § III, the distribution function for $|g|$ due to a random distribution of points all of the same mass is found with the aid of computer simulation. Once the present net gravitational acceleration is known, the present peculiar velocity can be calculated, given the cosmological density parameter Ω. In § IV, the expected range of velocities as a function of Ω is examined.

The tidal field of the net potential field gives rise to shear motion in bodies that are still expanding. These effects are

examined in § V along with the limits to the overdensities on large scales implied by measurements of supercluster rotation rates.

II. ANALYTIC DERIVATION OF MEAN SQUARED ACCELERATION

We can derive the gravitational acceleration at a given point due to randomly distributed mass clumps all of mass M_1 and at a number density of $N(M_1)$. If we know the mass function, i.e., number density for every mass range, then we can add stochastically the contributions due to different mass ranges.

The present gravitational acceleration on a supercluster due to another mass M_1 and distance R is

$$\Delta g_1 = \frac{GM_1}{R^2} . \tag{1}$$

The number of superclusters of mass M_1 between R and $R + dR$ is $4\pi R^2 N(M_1)dR$. The galaxy two-point correlation function falls below unity at scales greater than 5 h^{-1} Mpc (Peebles 1976), and the Abell cluster correlation function falls below unity at a scale length of ~ 25 h^{-1} Mpc (Bahcall and Soneira 1983), so Poisson statistics are suitable for a first-order approximation of the distribution of superclusters in space if a large fraction of all galaxies are contained in superclusters. As in all stochastic processes, with N acceleration vectors each of which has a magnitude of Δg_1, the square of the sum of the vectors is ${g_1}^2 = N(\Delta g_1)^2$.

The average value of ${g_1}^2$ per mass interval is found by multiplying $(\Delta g_1)^2$ for a given R with the number of mass centers with mass in the interval M_1 and $M_1 + dM_1$ at that distance and integrating over all distances,

$$\langle {g_1}^2 \rangle dM_1 = 4\pi N(M_1) G^2 {M_1}^2 dM_1 \int_{R_{\min}}^{R_{\max}} \frac{1}{R^2}\, dR$$

$$= 4\pi N(M_1) G^2 {M_1}^2 {R_{\min}}^{-1} dM_1 . \tag{2}$$

The integrand falls off fast enough that we need not consider general relativistic effects, and we can effectively take $R_{\max} = \infty$. The divergence at small R does not present a great difficulty since any two superclusters very close to one another rapidly fall together resulting in a single system with zero net peculiar motion. Also, we are interested only in accelerations correlated over the entire supercluster. For these calculations, $R_{\min}$ is arbitrarily taken to be the radius at which the internal fractional overdensity $\delta\rho/\rho$ reaches unity, with characteristic dimension assumed to be 20 h^{-1} Mpc. It is important to note the dependence of $\langle {g_1}^2 \rangle$ on number density and mass in equation (2). The distribution of the accelerations in the following sections has the same form as equation (2), but the constant 4π is replaced by a probability distribution.

To obtain the average squared acceleration due to a spectrum of masses, equation (2) is integrated over mass. It is, therefore, necessary to assume a form for $N(M)$. Assuming $N(M)$ is represented by a power law extending over at least one decade in mass with cutoffs at M_1 and M_2, then the expectation value of the squared acceleration is

$$\langle g^2 \rangle = 4\pi G^2 {R_{\min}}^{-1} N_0 {M_1}^2 \left(\frac{\alpha - 1}{\alpha - 3}\right) : \quad \alpha > 3 , \tag{3}$$

where N_0 is the total density given by $N_0 = N_0 = N_1 \int_{M_1}^{M_2} (M/M_1)^{-\alpha} dM$.

It is not highly informative to know only the expectation value of a distribution, and at times, it can be misleading. The median value of g^2, with certain probability distributions, can be much lower than $\langle g^2 \rangle$. For example, the addition of a shallow tail onto the high end of a distribution curve can greatly increase the expectation value while only slightly increasing the mode and median values. To make meaningful inferences from observed peculiar motions, the probability function of $|g|$ needs to be calculated.

III. PROBABILITY DISTRIBUTION OF NET ACCELERATION

The magnitude of the acceleration at a point due to a distribution of n point objects all of the same mass is given by

$$|g| = GM\left[\left(\sum_n \frac{x_n}{{R_n}^3}\right)^2 + \left(\sum_n \frac{y_n}{{R_n}^3}\right)^2 + \left(\sum_n \frac{z_n}{{R_n}^3}\right)^2\right]^{1/2} . \tag{4}$$

If we recast this into a form similar to that given for $\langle g^2 \rangle$ in equation (2),

$$|g| = AGMN^{1/2} {R_{\min}}^{-1/2} , \tag{5}$$

where the dimensionless random variable

$$A = N^{-1/2} {R_{\min}}^{1/2} [\textstyle\sum + \sum + \sum]^{1/2} .$$

The probability density for A, $P_N(A)$, can be evaluated and should change slowly with the ratio $R_{\min}/N^{-1/3}$, since it is constrained by the fact that

$$\int_0^\infty A^2 P_N(A) dA = 4\pi . \tag{6}$$

With the aid of a computer, N points (where N was usually greater than 50) were selected at random within a unit cube, but outside a smaller centrally located sphere. Choosing N and a value for $R_{\min}/N^{-1/3}$ determines $D_{\min}$, the radius of the central sphere. The set of random points was reselected 200 times. Statistics on the frequency of occurrence in discrete intervals of values of A were accumulated and the probability density $P_N(A)$ was, thereby, approximated along with its integrated probability function. The results are plotted in Figure 1.

The limiting case of $N^{-1/3} \gg R_{\min}$ can be represented by a slightly different expression which does not depend on $R_{\min}$:

$$|g| = A'GMN^{2/3} , \tag{7}$$

where $A' = N^{-2/3}[\sum + \sum + \sum]^{1/2}$. The probability distribution of A' is plotted in Figure 2 along with its integrated probability. It is enlightening to see that the general shapes of A' and A, for the values of $R_{\min}/N^{-1/3}$ used, are fairly similar, yet the shallow tail in the distribution of A' arising from very near mass points causes the mean of A' to be infinite.

Now, in adding up the contributions of various mass ranges, notice that each mass range has an associated number density given by a presumed mass function. Thus, each mass range contributes a probability density for $|g|$ of more or less similar shape except for the width, which goes as MN^β, where $\frac{1}{2} < \beta < \frac{2}{3}$. The probability density function for the sum of two independent random variables is the convolution of the probability functions of the random variables, so the net probability density for g^2 is the net convolution of all the distributions for g^2 due to different mass ranges. The width of the convolution of two such functions is approximately equal to the root of the sum of the squares of the widths of the original functions. Thus the distribution from a spectrum of masses is well approximated by merely considering the mass range with the maximum width or equivalently the greatest MN^β.

IV. VELOCITY DISTRIBUTION OF SUPERCLUSTERS

The specification of a scale sufficiently large that fractional density excesses are less than unity ensures that these pertur-

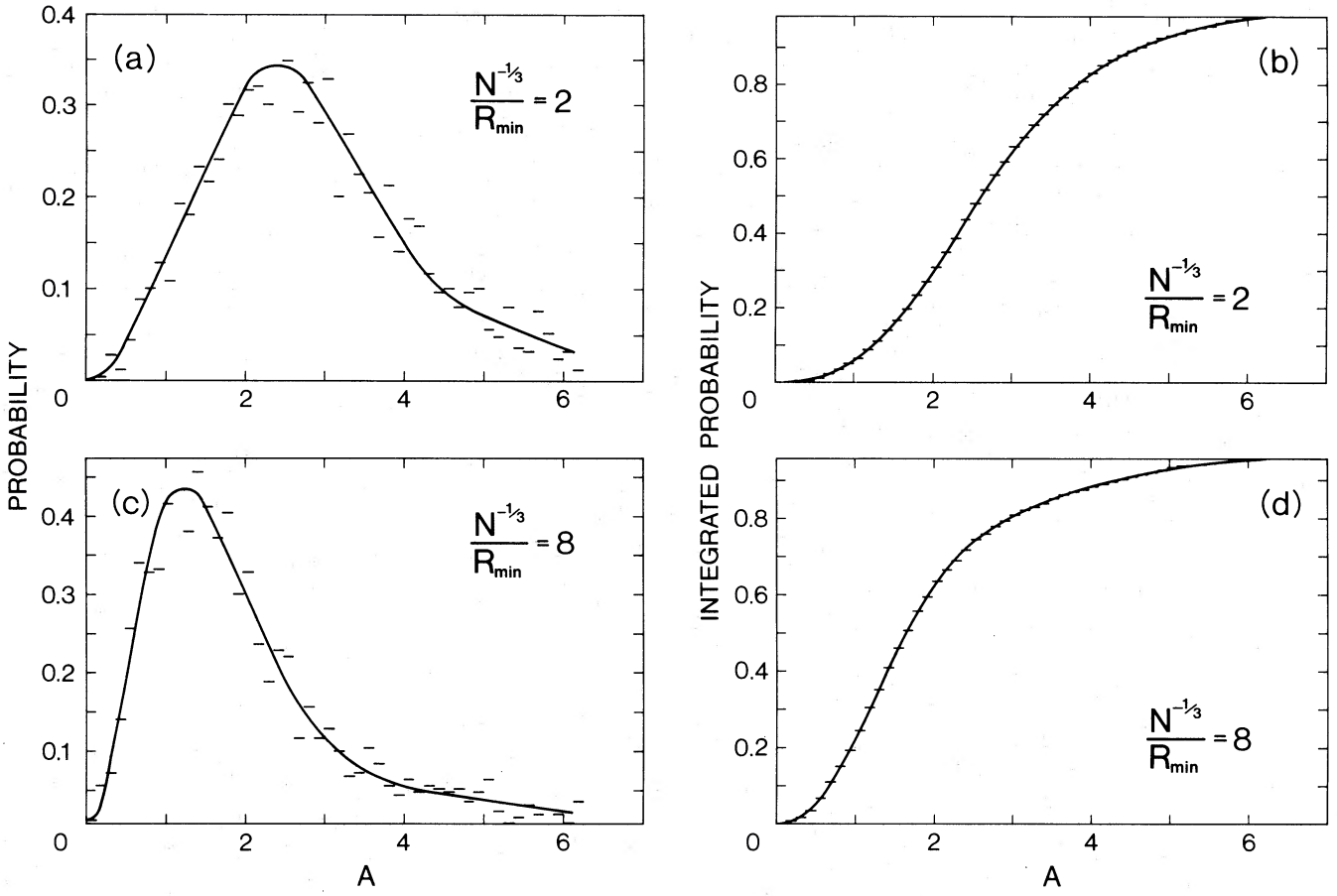

FIG. 1.—Probability per unit interval of A derived from Monte Carlo simulations of N equal mass points in a cube with (*a*) $R_{min} = N^{-1/3}/2$ and (*c*) $R_{min} = N^{-1/3}/8$. The integrated probability function of A with (*b*) $R_{min} = N^{-1/3}/2$ and (*d*) $R_{min} = N^{-1/3}/8$.

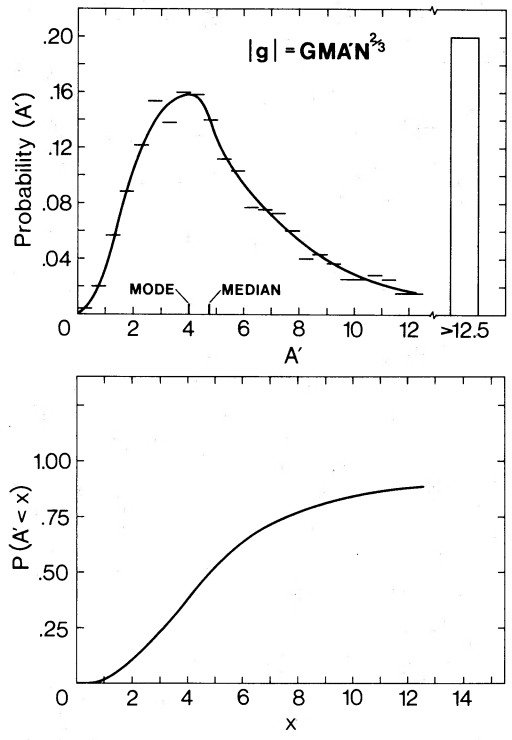

FIG. 2.—Probability function per unit interval of A' per unit interval and its integrated function.

bations have grown linearly. Accordingly, from the time of recombination until the present, density perturbations on this scale have merely been amplified with minor alteration in shape. The net gravitational field arising from these large-scale perturbations has changed only in amplitude with time; the direction of acceleration on such large-scale objects have remained fixed.

The cosmological relationship between present accelerations and peculiar velocities derived in linear perturbation theory is (Peebles 1980)

$$u_0 = \frac{2}{3}\frac{g_0}{H_0}\Omega^{-0.4}\,. \tag{8}$$

It is, however, the mass excesses above the mean density that contribute to g_0 instead of the total masses.

Redshift surveys of the large-scale space distribution (Gregory and Thompson 1978; Kirshner, Oemler, and Schechter 1979; Tarenghi *et al.* 1980; Gregory, Thompson, and Tifft 1981; Davis *et al.* 1982) reveal a substantial fraction of galaxies is situated in superclusters. Correspondingly large holes devoid of galaxies are also found. These holes also contribute to the net acceleration vectors since it is deviations from the mean which cause the peculiar motions. Incidentally, the presence of these holes should not be surprising. Small density perturbations grow in proportion to $t^{2/3}$ in early times for density deficits ($\delta\rho < 0$) as well as for excesses.

Combining equation (8) with equation (5) one obtains for the

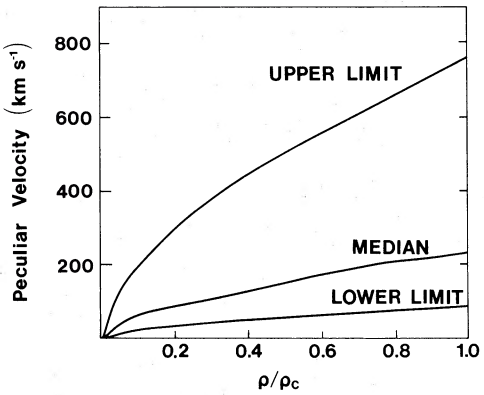

FIG. 3.—The probability functions of Fig. 1 were used in evaluating the upper limit (95%), median, and lower limit of the peculiar velocities of a sphere of radius 20 h^{-1} Mpc as a function of Ω assuming $R_{\min} = N^{-1/3}/3.2$.

peculiar motion of the spherical volume containing a fractional overdensity of unity

$$u_0 = \left(\frac{N^{-1/3}/R_{\delta=1}}{3.2}\right)^{-3/2}\left(\frac{R_{\delta=1}}{20\ h^{-1}\ \mathrm{Mpc}}\right)A\Omega^{0.6}\ 117\ \mathrm{km\ s^{-1}}\ , \tag{9}$$

where $h \equiv H_0/100$ km s^{-1} Mpc^{-1} and $R_{\delta=1}$ is the mean supercluster radius at which δ, the fractional density excess internal to R, reaches unity.

The combined number density of both superclusters and supercluster-sized voids is taken to be one per (63 h^{-1} Mpc)^3. There are eight known superclusters with $v < 10{,}000$ km s^{-1}—Hydra/Centaurus, Lynx/Ursa Major, Pisces/Perseus, Coma/A1367, A2199/2197, A2634/2666, Indus, and Virgo—which is the same as one per (80 h^{-1} Mpc)^3. The contribution to the velocity arising from large-scale density deficits or voids, which could be almost as great as the contribution arising from the superclusters, was accounted for by simply doubling the number density to give the combined number density.

Several superclusters with $v < 10{,}000$ km s^{-1} may still remain undiscovered for several reasons. There is a large section of the southern hemisphere sky that has not been thoroughly investigated because Abell's original catalog of clusters (Abell 1958) did not cover the whole sky. The plane of the Galaxy may hide superclusters within this velocity interval. Superclusters that are less conspicuous because they do not include rich clusters would likely have escaped detection. Therefore, it should be kept in mind that the actual number density of superclusters, especially inconspicuous superclusters of which the Local Supercluster is an example, may be considerably greater than 1 per (80 Mpc)^3.

The median and 95% upper and lower limits to the peculiar velocity of a 20 h^{-1} Mpc sphere as a function of the density parameter shown in Figure 3 demonstrate the range of velocities expected. The peculiar velocities vary as the inverse square root of the radius of the sphere. Less than 5% of the superclusters in a universe with mean density of 0.2 times critical density would have velocities greater than 300 km s^{-1}. On the other extreme, if the universe is closed or nearly so, then peculiar velocities greater than 200 km s^{-1} would be the norm. Improvements in velocity independent distance determinations (Tully and Fisher 1977; Aaronson, Mould, and Huchra 1980; Bottinelli *et al.* 1980) may soon make this range of peculiar velocities discernible in the nearby superclusters.

V. TIDAL EFFECTS

It is also worthwhile to investigate the tidal effects of a random distribution of similar masses. The tidal acceleration at a point $\boldsymbol{r}$ within a supercluster due to another supercluster at a distance D is

$$\boldsymbol{g}^{\mathrm{tidal}} = \left(\frac{3\boldsymbol{R}(\boldsymbol{R}\cdot\boldsymbol{r})}{R^2} - \boldsymbol{r}\right)\frac{G\delta M}{R^3}\ , \tag{10}$$

or in component notation $g_i^{\mathrm{tidal}} = E_{ij}r_j$, where (Olson 1980)

$$E_{ij} = \left(\frac{3R_iR_j}{R^2} - \delta_{ij}\right)\frac{1}{R^3} \times G\delta M\ . \tag{11}$$

For a random distribution one needs to sum each of the elements of E_{ij} over n particles. A dimensionless parameter was formed for the Monte Carlo simulations:

$$B_{ij} = N^{-1/2}R_{\min}{}^{3/2}\sum_n\left(\frac{3R_i{}^nR_j{}^n}{R_n{}^2} - \delta_{ij}\right)\Big/R_n{}^3\ . \tag{12}$$

Figure 4 demonstrates the distribution of the off-diagonal elements B_{ij} due to a random distribution of points outside $R_{\min}$. The tidal tensor is then

$$E_{ij} = B_{ij}G\delta MN^{1/2}R_{\min}{}^{-3/2}\ . \tag{13}$$

a) *Shear Motions*

The off-diagonal components of the tidal tensor result in nonradial or shear motions which are given by the integration over time of the tidal acceleration

$$v = \int E_{ij}r_j\,dt\ . \tag{14}$$

For early times, $a \propto t^{2/3}$ and the strength of the tidal field $E_{ij} \propto [\rho(<R) - \rho(R)] \propto a^{-3}[\delta(<R) - \delta(R)] \propto t^{-4/3}$. At late times in a low density universe ($a_0/a < (\Omega_0{}^{-1} - 1)$; see Peebles 1980, p. 51), $a \propto t$ and $\delta =$ constant, so $E_{ij} \propto t^{-3}$. In the expanding outer regions of a supercluster that is bound or nearly bound, $r \propto t^{2/3}$ until the present. Let us take, as an approximation, $t = t_0/(\Omega_0{}^{-1} - 1)$ as the time at which a sudden transition from early to late time behavior occurs; then equation (14) is easily integrated to yield

$$\frac{v_0}{r_0} = E_{ij}{}^0t_0 \times \begin{cases} 3 & :\Omega_0 \sim 1 \\ \dfrac{15}{4}\,(\Omega_0{}^{-1} - 1)^{4/3} - 1 & :\Omega_0 \ll 1\ . \end{cases} \tag{15}$$

The smaller universal density parameter, the greater the shear velocity for a given present-day tidal field strength.

If we again take into account negative as well as positive density excesses, the shear motion today in objects that are still in the linear regime of growth is

$$\frac{v_0}{r_0} \geq \left(\frac{\delta M}{10^{15}\ M_\odot}\right)\left(\frac{N^{-1/3}}{63\ h^{-1}\ \mathrm{Mpc}}\right)^{-3/2} \times \left(\frac{R_{\min}}{20\ h^{-1}\ \mathrm{Mpc}}\right)^{-3/2} 3\ h^2B_{ij}\ \mathrm{km\ s^{-1}\ Mpc^{-1}}\ . \tag{16}$$

Taking 16.8 Mpc (Tully and Shaya 1984) for our distance from the center of the Local Supercluster and values of unity for the terms in brackets, shear flow of about 50 h^2 km s^{-1} at our position is predicted, since the median value of B_{ij} is approximately unity. An upper limit (95% lower limit of B_{ij} is 0.1) of $\sim 3 \times 10^{16}\ h^{-2}\ M_\odot$ for the excess masses of our neighboring

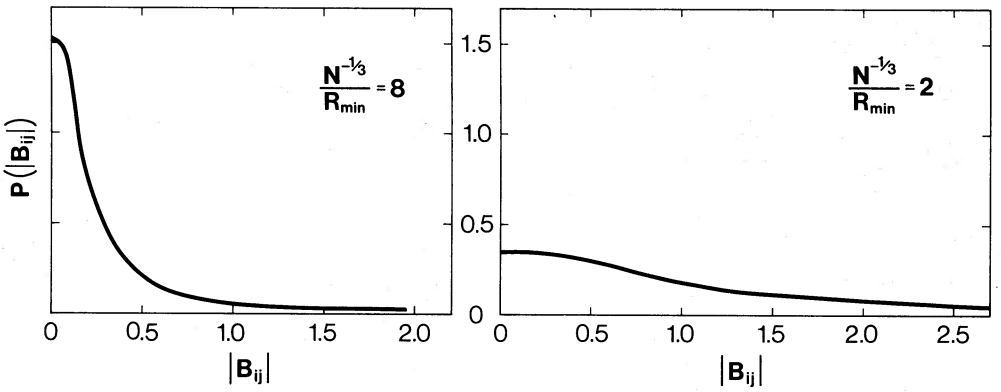

FIG. 4.—Probability per unit interval for the off-diagonal tidal field tensor B_{ij} in a random distribution of equal mass points and (*a*) $R_{min} = N^{-1/3}/8$, (*b*) $R_{min} = N^{-1/3}/2$.

superclusters is implied if the shear motions in the Local Supercluster are under 150 km s^{-1} and $\Omega = 1$. The upper limit is reduced to $\sim 1 \times 10^{15}\ h^{-2}\ M_\odot$ if $\Omega_0 = 0.1$. The lower limit for δM (95% upper limit of B_{ij} is 2.5) is $1.2 \times 10^{15}\ h^{-2}\ M_\odot$ with $\Omega = 1$ if the shear motions are greater than 150 km s^{-1}. The lower limit is reduced to $4 \times 10^{13}\ h^{-2}\ M_\odot$ if $\Omega = 0.1$. A higher number density would, of course, reduce these mass limits.

Shear velocities of several hundred km s^{-1} are measurable in other superclusters by modern techniques; however, large numbers of velocity measurements for each supercluster are required. Measurements of the amplitude of shear motion within several superclusters would provide a measure of the average mass excess in superclusters.

b) Tidal Distortion

Tidal forces can produce distortions of the velocity field which in turn result in increases in asphericities. For the case in which two or three proto-superclusters were close enough to partially merge, a particularly aspherical system arises. A Hubble time is not long enough for these large systems to fully merge and relax into a spherical system. For this reason, calculations of tidal distortion should include the influence of superclusters closer that D_{min}. The assumption of a constant geometry here strongly underestimates the influence of superclusters with separation velocities that depart significantly from Hubble flow.

When no minimum distance is specified, the tidal field tensor can be expressed as

$$E_{ij} = B_{ij}' G N \delta M \ . \tag{18}$$

It is advantageous in examining tidal distortion caused by a random distribution of gravitating systems to rotate the coordinate axes so that they are aligned with the directions of maximum stress and compression. The tidal tensor, being symmetric, can always be diagonalized, an operation equivalent to performing the desired rotations. The distribution of the three trace elements of the diagonalized tensor for B_{ij}' are presented in Figure 5.

Strong tidal influences occur if the acceleration of the tidal stress is nearly equal to the self-gravitational accelerations. Equality of these quantities, implying tidal disruption, occurs when

$$E_{xx}^{\text{Roche}} = \frac{GM}{r^3} = \frac{4}{3}\pi G\langle\rho\rangle \ . \tag{18}$$

The limit on B_{xx}' for disrupting a system of mean internal density $\langle\rho\rangle$ is

$$B_{xx}' = 32\,\frac{\langle\rho\rangle}{\bar{\rho}}\left(\frac{N^{-1/3}/R_{\delta=1}}{3.2}\right)^3 \tag{19}$$

If $N^{-1/3}/R_{\delta=1}$ is equal to 3.2, in about 10% of all superclusters, the tidal field strength from neighboring superclusters is greater than half of that required to tear apart the supercluster at the contour where $\langle\rho\rangle/\bar{\rho} = 1$. In one-third of all superclusters, the strength of the tidal field is greater than one-fourth of the critical level for disruption.

VI. DISCUSSION

A peculiar velocity of several hundred km s^{-1} for the Local Supercluster has been inferred from a comparison of the dipole measurements of the background radiation with the motion of our galaxy relative to galaxies of the Local Supercluster. A natural explanation for this motion is found when the summed gravitational attraction of nearby superclusters is considered. However, the "zone of avoidance" may completely hide nearby superclusters and surely obscures parts of known ones. Interestingly, the direction of this peculiar motion is close to that of Hydra/Centaurus, the nearest large supercluster. Maps of the Local Supercluster (Tully 1982) show that the longest axis of our supercluster is pointing roughly in the direction of

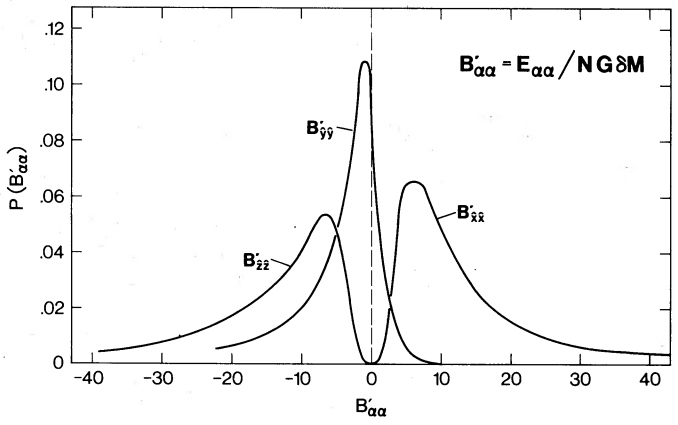

FIG. 5.—Probability per unit interval for the nonshearing trace elements of the diagonalized B_{ij}' tensor. B_{xx}' is the greatest valued of the three elements, B_{zz}' is the lowest one, and B_{yy}' is the intermediate one.

the Hydra/Centaurus Supercluster. Perhaps this supercluster had an influence that determined the axes of collapse of the Local Supercluster as well as its direction of motion.

Hydra/Centaurus is known to contain three clusters of approximately Virgo Cluster size: Antlia at a redshift of $v = 2600$ km s^{-1} and with velocity dispersion $\sigma = 609$ km s^{-1}; Hydra I (A1060) at $v = 3346$ km s^{-1} and with $\sigma = 786$ km s^{-1}; and Centaurus at $v = 3261$ km s^{-1} and with $\sigma = 945$ km s^{-1} (Yahil and Vidal 1977). The distance to this supercluster from the Virgo Cluster is roughly twice the distance between the Virgo Cluster and the Local Group. Thus, it would not be surprising if the peculiar velocity of the Local Supercluster due to Hydra/Centaurus alone were nearly as great as the peculiar velocity of the Local Group due to the Virgo Cluster. A proper analysis of the cause of the motion of the Local Supercluster would necessarily take into account the influence of other nearby superclusters.

The statistical approach formulated here has been forced on us by our limited knowledge of nearby superclusters. The specification of the mass function for a random distribution of superclusters is needed to determine the probability density distribution for the peculiar velocity of a supercluster. Assuming there is a limited mass range for superclusters, limits to that mass range can be set, given the peculiar velocity of at least one supercluster. With $N^{-1/3}/R_{\delta=1} = 3.2$, which corresponds to 0.065 of the mass of the universe in supercluster excesses, the 95% upper limit probability to the peculiar velocity of a supercluster is ~ 760 km s^{-1} for a critical density universe, and this value drops to 300 km s^{-1} for $\Omega = 0.2$. Determination of deviations from Hubble flow of nearby superclusters could be used to better determine the density of the universe.

Shear velocities and distortional velocities are predicted to be the same magnitude as the peculiar velocity of the system. Although the shear motions are not important for centrifugal dynamical effects, they might be observable in other superclusters. Measurements of the rotation of the Local Supercluster (de Vaucouleurs 1958; Aaronson *et al.* 1982) find a shear flow of ~ 150 km s^{-1} at the Local Group position. For this velocity, a 95% upper limit to the mass excess in superclusters is $3 \times 10^{16}\ h^{-2}\ M_{\odot}$. These calculations assume that asphericity is of primordial origin, in which case a lack of rotation in clusters and superclusters can set cosmologically significant upper limits to the mass in superclusters.

A few superclusters will be strongly aspherical because they are the merger of two or three clusters, which were initially very close. Such systems would surely remain highly aspherical for longer than a Hubble time and would be subject to large torques from the tidal fields of neighbors.

It is, however, conceivable for a high degree of asphericity to have been produced without necessarily inducing much rotation. If a substantial fraction of the mass is clumped into superclusters, then the majority of superclusters are undergoing strong tidal interactions. If the tidal distention dominates the self-gravitation, it will define the shapes of superclusters. The resulting configuration will be locked to the prevailing tidal field. This very basic physical process must be going on to some degree and may explain at least in part the bridges and "cell-like" structure of groups of superclusters (Giovanelli and Haynes 1982; Einasto, Joeveer, and Saar 1980; Chincarini, Rood, and Thompson 1982).

Guidance and encouragement from Brent Tully are gratefully appreciated. The efforts of Laird Thompson and Alan Stockton to improve the manuscript were of great benefit. Financial support was provided by the Honolulu Chapter of the Achievement Rewards for College Scientists Foundation and by NSF grant AST 82-03971.

REFERENCES

Aaronson, M., Huchra, J., Mould, J., Schechter, P., and Tully, R. B. 1982, *Ap. J.*, **258**, 64.
Aaronson, M., Mould, J., and Huchra, J. 1980, *Ap. J.*, **237**, 655.
Abell, G. 1958, *Ap. J. Suppl.*, **3**, 211.
Bahcall, N., and Soneira, R. 1983, *Ap. J.*, **270**, 20.
Binggeli, B. 1982, *Astr. Ap.*, **107**, 338.
Bottinelli, L., Goguenheim, L., Paturel, G., and de Vaucouleurs, G. 1980, *Ap. J. (Letters)*, **242**, L153.
Chincarini, G., and Rood, H. J. 1979, *Ap. J.*, **230**, 648.
Chincarini, G., Rood, H. J., and Thompson, L. A. 1981, *Ap. J. (Letters)*, **249**, L47.
Clutton-Brock, M., and Peebles, P. J. E. 1981, *A.J.*, **86**, 1115.
Davis, M., Huchra, J., Latham, D. W., and Tonry, J. 1982, *Ap. J.*, **253**, 423.
de Vaucouleurs, G. 1958, *A.J.*, **63**, 253.
de Vaucouleurs, G., Peters, W. L., Bottinelli, L., Goguenheim, L., and Paturel, G. 1981, *Ap. J.*, **248**, 408.
Efstathiou, G., and Jones, B. J. T. 1979, *M.N.R.A.S.*, **186**, 133.
Einasto, J., Joeveer, M., and Saar, E. 1980, *M.N.R.A.S.*, **193**, 353.
Giovanelli, R., and Haynes, M. 1982, *A.J.*, **87**, 1355.
Gregory, S. A., and Thompson, L. A. 1978, *Ap. J.*, **222**, 784.
Gregory, S. A., Thompson, L. A., and Tifft, W. G. 1981, *Ap. J.*, **243**, 411.
Kirshner, R. P., Oemler, A., and Schechter, P. L. 1979, *A.J.*, **84**, 951.
Olson, D. 1980, *Ap. J.*, **236**, 335.
Peebles, P. J. E. 1969, *Ap. J.*, **155**, 393.
———. 1976, *Ap. Space Sci.*, **45**, 3.
———. 1980, *The Large-Scale Structure of the Universe* (Princeton: Princeton University Press).
Tarenghi, M., Chincarini, G., Rood, H., and Thompson, L. A. 1980, *Ap. J.*, **235**, 724.
Thuan, T., and Gott, J. 1977, *Ap. J.*, **216**, 194.
Tully, R. B. 1982, *Ap. J.*, **257**, 389.
Tully, R. B., and Fisher, J. R. 1977, *Astr. Ap.*, **54**, 661.
Tully, R. B., and Shaya, E. B. 1984, *Ap. J.*, in press.
Yahil, A., and Vidal, N. V. 1977, *Ap. J.*, **214**, 347.

E. J. SHAYA: Institute for Astronomy, University of Hawaii, 2680 Woodlawn Drive, Honolulu, HI 96822